



Contents lists available at ScienceDirect

Chinese Chemical Letters

journal homepage: www.elsevier.com/locate/ccllet

Editorial

Oral delivery of insulin by barbed microneedles actuated by intestinal peristalsis



Oral formulations are always preferred to injections due to the advantages of high patient compliance, no biohazardous needle waste, and low requirements for administration skills. However, the presence of multiple gastrointestinal (GI) barriers, including extreme gastric acidity and a broad pH gradient, digestive enzymes, thick and variable mucus layers, and tight junctions in the enteric epithelia, restricts the rate and extent of oral absorption. Only active ingredients with favorable physicochemical properties, for example, small molecules with balanced hydrophobicity and hydrophilicity, are able to achieve adequate bioavailability. For biologic drugs such as peptides, proteins, nucleic acids, and antibodies, parenteral administration, especially *via* injection, is the method of choice because biologics are readily deactivated once exposed to the harsh GI environment and cannot be transported across the mucosal and epithelial barriers. Current noninvasive approaches involving the use of permeation enhancers, enzyme inhibitors, carrier systems, and mucoadhesive or muco-penetrating strategies and microdevices only achieve limited oral bioavailability [1].

Despite the stereotyped preconception of noninvasiveness for oral delivery, pioneer invasive oral approaches have been tested recently to deliver biologics directly to the systemic circulation, trespassing the enteric epithelial barriers [2–4]. It was reported that injection in the GI tract by a one-shot needle or microneedle (MN) array achieved a peak plasma level of insulin within 30 min and an oral bioavailability of more than 10% compared with parenteral injection [2,3]. Usually, injection is triggered by precompressed springs or balloons poised for ejection or expansion or by external magnetic forces [2–4]. Although they are ingenious in design, each robot has its own drawbacks. For instance, a one-shot robot driven by springs or balloons may be subject to high ratios of misactuation, while a magnetic field-controlled robot requires sophisticated manipulation and suffers from magnet-induced distress. More importantly, safety concerns are raised regarding the use of metal springs, nondegradable elastomers or magnetic particles in formulations. Thus, there is always a motivation to engineer exquisite delivery systems or devices with excellent safety profiles to implement precise and punctual injection within the GI tract.

Recently, in *Science Advances*, Gao and colleagues at Tsinghua University reported a tactfully orchestrated barbed MN robot, which was actuated by natural intestinal peristalsis rather than external triggers, and achieved an oral insulin delivery efficacy of 23.6% compared to that of subcutaneous injection in minipigs (Fig. 1) [5]. According to the authors' rhetoric, the idea was

inspired by the porcupinefish's ability to inflate and marshal its spines for defense whenever endangered (Figs. 1A and B). The barbed MNs were engineered on stretchable hydrogel membranes (Figs. 1C and D). Upon imbibition of water, the MN robot could swell by 20 times in volume (Fig. 1E) with microneedles oriented vertically outward on the robot surfaces (Figs. 1F and G). Following oral administration in enteric capsules, the MN robot was released into the small intestine and rapidly imbibed water to swell to its full size (Fig. 1H). Upon peristaltic contraction, the barbed MNs were injected into the enteric mucosa and then detached in response to peristaltic relaxation (Fig. 1I). The dislodged hydrogel backing was subsequently disintegrated and expelled from the body.

The barbed MN robot was fabricated by a double-mold process (Fig. 2A), with the drug insulin loaded into the barbed needle tips (Figs. 2B and C). Fig. 2B schematically illustrates the variations in peristaltic forces and lumen diameter during the contraction/relaxation rhythms. Dislodging of the barbed tips occurred after injection of the MNs into the mucosa by peristaltic contraction (Fig. 2B). In an *in vitro* gel model simulating mucosa, dislodging of insulin-loaded barbs was successfully recorded (Fig. 2C, middle), but unfortunately, this process was not observed *in vivo*, and detached barbs were only observed on the surface of intestinal mucosa (Fig. 2C, below). By adjusting the ratio of the membrane mixture (PVA and AAm), a stretchable membrane with a stretch degree of 50% was obtained. After the addition of the osmotic agent citric acid to the internal swelling agent (sodium carboxymethyl cellulose), the volume could swell by 20 times. By doping PEG in the barbed structure, drug release could be accelerated to more than 50% within 3 h *in vitro*. Each MN patch was loaded with 0.5 mg of insulin in 126 tetragonal barbs (height, 800 μm ; underside length, 500 μm), for a total of 1.0 mg in a single MN robot.

Based on their design, the volume of the robot in the swelling equilibrium state directly determines the peristaltic contraction force acting on it, which significantly affects the penetration efficiency of the drug-loaded MNs. First, they customized pressure sensors of three diameters to measure the peristaltic pressure in Bama minipigs in real time to optimize the size of the swelling MNs, which may suffer the same contraction force as the sensor with the same diameter. In the swelling equilibrium state, when the diameter of the MN robot reaches 14 mm, a single MN will withstand an intestinal pressure of 10.5 mN, which is 4 times greater than the required penetration force in the literature. Both *in vitro* and *in vivo* penetration results confirmed the penetration

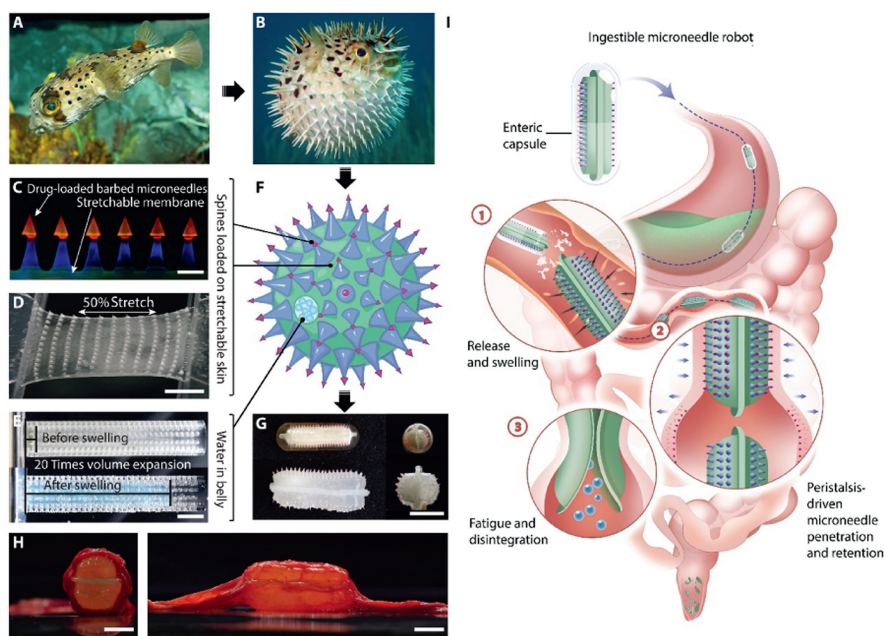


Fig. 1. (A, B, F) The idea of a barbed MN robot is inspired by the ability of a porcupinefish to inflate and marshal its spines for defense. (C) Fluorescently stained MNs indicating the MN bodies and barbs. (D) Stretchable membrane displaying 50% stretch. (E) Volume expansion by 20 times following imbibition of water. (F) Front and side views of a pre- and post-swelling NM robot. (G) Front and side views of a swollen MN recovered from minipig intestine. (H) Front and side views of a swollen MN recovered from minipig intestine. (I) Schematic illustration of the rationale of the barbed MN robot. Copied with permission [5]. Copyright 2024, AAAS.

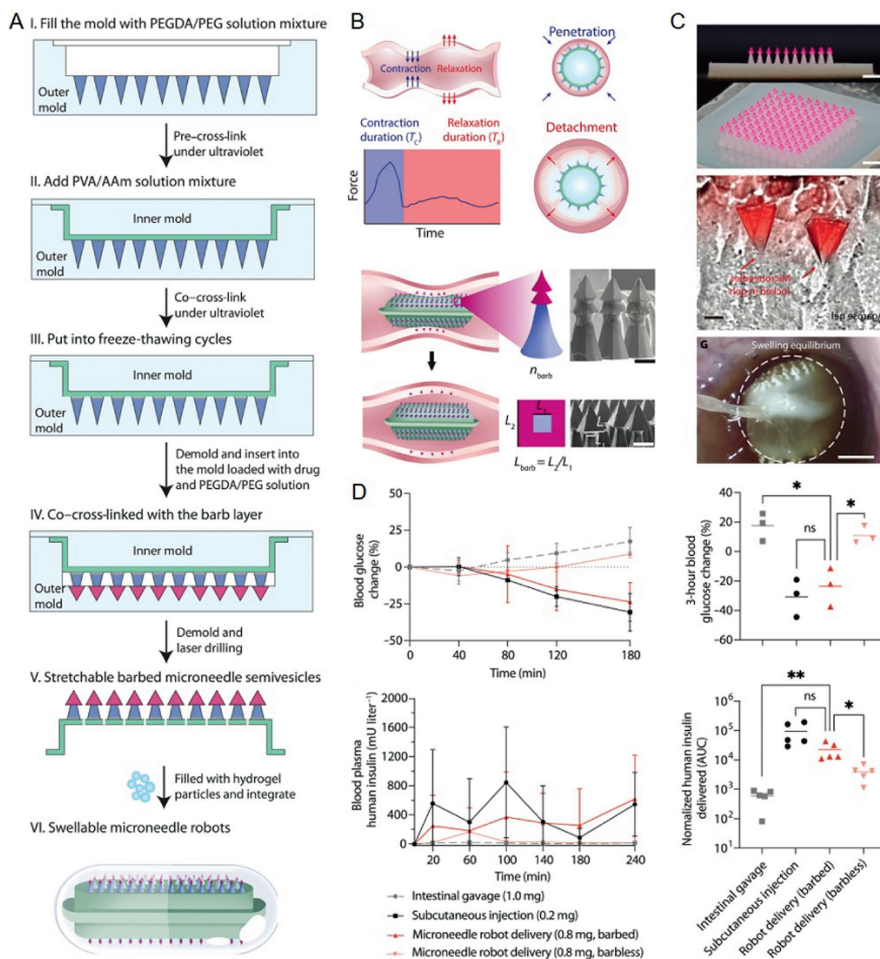


Fig. 2. (A) Double-mold procedures for the fabrication of barbed MN robots. (B) Schematic illustration of the variations in peristaltic forces and lumen diameters during contraction/relaxation rhythms and the dislodging of the barbed tips. (C) MNs with barbs (red tip) on stretchable membrane, dislodging of barbed tips in gels simulating mucosa, and an image revealing the swelling state of the robot in the small intestine. (D) Hypoglycemic effect and blood insulin levels following oral administration of the MN robots. Adapted with permission [5]. Copyright 2024, AAAS.

efficiency of the MN robot. For efficient delivery, the drug-loaded MNs need to be retained in the intestinal wall after penetration because the intestine undergoes a longer relaxation phase after contraction in a single peristaltic rhythm. Notably, the retraction force was greater than the connection force of the barbed tips with the robot, and the barbed tips were easily separated from the robot and trapped inside the intestinal tissue during the peristaltic relaxation phase. After 20 simulated peristaltic contraction/relaxation cycles, up to $93.5\% \pm 2.8\%$ of the tips were separated from the robot and retained in the intestinal tissue *ex vivo*. During the 1-h penetration/retraction cycles, the barbed MNs released up to 51.5% of the drugs (fluorescent dyes) in the tissue, while the barbless MNs released only 11.9% because of a lack of the dislodging process. The barbed structures of this MN device play a key role in achieving tissue retention and sustained drug release through peristaltic relaxation.

Subsequently, the drug delivery efficacy of the MN robot was confirmed in minipigs. The robots were delivered directly into the duodenum to avoid long gastric emptying times, and the robots were continuously observed using a gastroscope. Once inside the intestine, the enteric capsule shell is dissolved, and the MN robots begin to swell and interact with the intestine. The robotic delivery device achieved a 23.6% decrease in blood glucose within 180 min, which was comparable to the 30.7% decrease achieved by subcutaneous injection (Fig. 2D). The gavage control groups did not show obvious decreases in blood glucose. Pharmacokinetic studies confirmed that the robotic delivery method achieved high-dose insulin delivery comparable to subcutaneous injection, with a relative bioavailability of 23.6% (Fig. 2D). Notably, the hypoglycemic effect or bioavailability in the barbed group was significantly greater than that in the barb-free group (4.1%), which confirmed the importance of the barbed structure in MN design for efficient drug delivery. Moreover, the materials used to fabricate the MN robots showed good biocompatibility *in vitro* biocompatibility tests. No intestinal obstruction was observed during delivery or subsequent health monitoring in the minipigs, and no intestinal bleeding or perforation was observed through MN penetration.

In summary, the MN robot has been validated to be effective and safe for the oral delivery of insulin, holding promise as a new platform for oral biological drug delivery. However, there are still some issues that need further investigation. As the MN robot is actuated by intestinal peristalsis, the inter-individual variation in gastric emptying time may present as an important factor that determines the onset time of treatment. If it takes too long for the robot to reach the intestine, for example, 4–5 days as observed in this study, delayed delivery of insulin would be of little practical significance. Moreover, it may be difficult to ensure the penetration depth of MNs into the intestinal walls, which affects the absorption pathways and drug delivery efficiency. Additionally, the long-term stability of unstable insulin was not evaluated, and the

in vivo evaluation on delivery efficiency was carried out in healthy minipigs rather than diabetic ones.

Declaration of competing interest

The authors declare that they have no known competing financial interests or personal relationships that could have appeared to influence the work reported in this paper.

The author Wei Wu is an Associate Editor for *Chinese Chemical Letters* and was not involved in the editorial review or the decision to publish this article.

CRediT authorship contribution statement

Qin Yu: Writing – original draft, Visualization. **Haisheng He:** Visualization, Validation. **Jianping Qi:** Visualization. **Yi Lu:** Validation. **Wei Wu:** Writing – review & editing, Supervision, Project administration, Conceptualization.

Qin Yu

Shanghai Skin Disease Hospital, Tongji University School of Medicine,
Shanghai 200443, China

Key Laboratory of Smart Drug Delivery of MOE, School of Pharmacy,
Fudan University, Shanghai 201203, China

Haisheng He

Key Laboratory of Smart Drug Delivery of MOE, School of Pharmacy,
Fudan University, Shanghai 201203, China

Jianping Qi, Yi Lu, Wei Wu*

Shanghai Skin Disease Hospital, Tongji University School of Medicine,
Shanghai 200443, China

Key Laboratory of Smart Drug Delivery of MOE, School of Pharmacy,
Fudan University, Shanghai 201203, China

*Corresponding author.

E-mail address: wuwei@shmu.edu.cn (W. Wu)

Received 20 March 2024

Revised 11 April 2024

Accepted 14 April 2024

Available online 15 April 2024

References

- [1] L. Li, S. Chunta, X. Zheng, et al., *Chin. Chem. Lett.* 35 (2024) 108662.
- [2] A. Abramson, E. Caffarel-Salvador, M. Khang, et al., *Science* 363 (2019) 611–615.
- [3] A.K. Dhalla, Z. Al-Shamsie, S. Beraki, et al., *Drug Deliv. Transl. Res.* 12 (2022) 294–305.
- [4] X. Zhang, G. Chen, X. Fu, et al., *Adv. Mater.* 33 (2021) e2104932.
- [5] X. Gao, J. Li, J. Li, et al., *Sci. Adv.* 10 (2024) ead7067.